



Investigation on the influence of weld position on the deformation behavior of welded tube during free bending process

Cheng Cheng^{1,2,3} · Chao Pan¹ · Xueshan Bai³ · Chunmei Liu¹ · Xunzhong Guo¹

Received: 2 December 2021 / Accepted: 8 February 2022 / Published online: 19 February 2022
© The Author(s), under exclusive licence to Springer-Verlag London Ltd., part of Springer Nature 2022

Abstract

The plastic deformation behavior of welded tube is affected by the non-uniform distribution of the mechanical properties of welded tube during the free bending process. To explore the influence of weld position on the forming quality and axis dimensional accuracy of welded tube, the free bending experiment and numerical simulation of welded tube were conducted in this paper. First, the principle of free bending was theoretically deduced and the stress distribution of bent tube was analyzed. Then, the hardness test and uniaxial tensile test were conducted to obtain the mechanical properties of weld zone and parent zone of welded tube. The material strength in the weld zone of welded tube is significantly higher than that in the parent zone. Finally, the free bending experiment and numerical simulation with different weld positions were carried out, and the influence of weld position on the bending radius, cross-sectional distortion, and wall thickness of bent tube was discussed. All these findings advance the insight into the free bending deformation behavior of welded tube and help to improve the forming quality of welded tubes and facilitate the application of free bending technology in welded tube.

Keywords Welded tube · Free bending · Non-uniform mechanical properties · Forming quality · Numerical simulation

1 Introduction

Metallic tube components are widely used in various industrial fields such as aviation, aerospace, nuclear energy engineering, and automobile, due to their lightweight, high-strength, and low energy consumption [1]. The welded tubes, as a typical metallic tube component, are becoming more widespread in multitudinous industries owing to the low cost, short production period, and great variety [2]. At present, a straight piece of welded tube needs to be deformed to a selected bending radius and angle according to practical

requirements. The traditional bending technologies, such as rotary-draw bending [3], tension-bending [4], and roll bending [5], were mainly used to bend the welded tube. However, with the developing trend of product customization, the demand for the bent tube component with small batch and complex configuration is increasing, as indicated by Yang et al. [6]. It is difficult for the abovementioned traditional bending technologies to realize the integral forming of welded tube with complex spatial shape. The free bending technology can realize the one-step forming of complex bent tube without changing the bending die, as discussed by Gantner et al. [7], and this technology shows great potential in the field of welded bent tube manufacturing.

In recent years, numerous studies on the free bending of aluminum alloys and stainless steel tubes have been carried out. Wu et al. [8] proposed a new theoretical model to describe the springback behavior of pure aluminum spatial tube with different loading modes and hardening materials during free bending process, and found that the radii and angles of bent tube both increase accordingly with increasing loading index k . Beulich et al. [9] developed a simplified simulation model for the free bending of aluminum alloy tube with a mandrel located inside the tube. The model was verified by surface measurements of a two-dimensional

✉ Cheng Cheng
c_cheng@nuaa.edu.cn

✉ Xunzhong Guo
guoxunzhong@nuaa.edu.cn

¹ College of Material Science and Technology, Nanjing University of Aeronautics and Astronautics, Nanjing 211100, People's Republic of China

² State Key Laboratory of Digital Manufacturing Equipment and Technology, Huazhong University of Science and Technology, Wuhan 430074, People's Republic of China

³ Shenyang Aircraft Corporation, Shenyang 110850, People's Republic of China

bending test. Aiming at the bending process of aluminum alloy tube, He et al. [10] established a 3D elastic–plastic finite element model and a wrinkling energy prediction model under multi-die constraints. To accurately predict the geometric size of the complex bending tubular components during free bending process, Guo et al. [11] proposed a new method to establish the relationship between the deflection of bending die (U) and bending radius (R) of aluminum alloy circular tube by conducting the sensitivity analysis of material parameters. Currently, most studies on the free bending technology are based on the seamless tubes, but few scholars have studied the free bending deformation behavior of welded tubes.

During the free bending process, the plastic deformation zone of tube is in a less constrained state. The small changes in material parameters will have a significant impact on the forming quality and geometric dimension of the bent tube. Due to the obvious difference in mechanical properties between the weld zone and parent zone of welded tube, the plastic deformation behavior of welded tube is more complicated during the free bending process. At present, the research on the bending deformation behavior of welded tube is mainly based on the traditional bending process. Ren et al. [12] investigated the constraining effects of the weld and heat-affected zone (HAZ) on the tube bend formability of the QSTE340 welded tube by the NC rotary draw bending (RDB) tests and finite element simulation. It was found that the weld and HAZ materials have obvious constraining effects on the strain distributions in weld and HAZ when the weld line is located on the outside and inside of the bent tube. In addition, the effect of the weld on the strain distribution of the tube during NC bending process was also explored by Ren et al. [13]. The findings suggest that the thickness strain decreases obviously in the weld region when the weld line is located on the outside and inside. Liu et al. [14] established the FE model of RDB of QSTE700 rectangular welded tube considering weld zone and corner and concluded that the wrinkling height of inner flange and side wall increases with the weld zone. Zhan et al. [15] took the continuous variations of the weld material properties, the anisotropic parameter, and the weld position into consideration in the analytical springback model. The springback angle after bending of the QSTE340 welded tube could be accurately predicted by the abovementioned model.

The material properties of seamless tube are evenly distributed along the cross-section; there are many theoretical and experimental studies on the free bending of seamless tubes. However, the influence of the distribution of material properties of welded tube on the free bending deformation behavior is complicated, and related research on welded tube is considerably limited. To accurately characterize the mechanical properties of weld zone and parent zone of welded tube, it is necessary to establish an accurate and continuous constitutive model across the

cross-section of welded tube. Khalfallah [16] proposed an efficient method to obtain plastic deformation behavior of welded tubes and the constitutive model parameters of weld bead and HAZ regions were determined by tensile tests, mixture rules, and microhardness tests. Likewise, Xing et al. [17] developed a new method for establishing a continuous constitutive model of welded metals via the relationship among the flow stress, microhardness, and weld shape. The continuous variation in flow stress across these zones can be characterized by the method. To accurately simulate the deformation behavior of welded steel tube during hydroforming process, the welded tube was modeled as two material system including weld zone and base metal region, whose stress–strain curves could be described by the mixture rule, as presented by Omar et al. [18]. To predict the fracture of welded tube, Jang et al. [19] established the constitutive model of the weld zone by the mixture rule and the flow stress of the weld was estimated according to the hardness ratio. Additionally, Liu and Liu [20] analyzed the cross-sectional deformation of thin-walled heterogeneous rectangular welded tubes in rotary draw bending process by considering different yield criteria. The anisotropic parameters of Hill'48 and Barlat'89 yield criteria of parent zone and weld zone were determined by using the digital image correlation test.

Since the material strength in the weld zone of welded tube is different from that in the parent zone, it is necessary to consider the influence of the non-uniform distribution of material properties on the free bending deformation behavior of welded tube. For this purpose, the free bending mechanism of welded tube was re-derived and the mechanical constitutive relationships of Q345 welded tube were determined by the hardness test, uniaxial tensile test, and mixed criterion method. The free bending experiments of welded tubes were carried out and the corresponding numerical simulation method was developed. The influence of weld position on U - R relationship, cross-sectional distortion, and wall thickness distribution was studied in detail. Finally, to improve the forming quality and axis dimensional precision of welded tube in the free bending process, the weld position needs to be carefully considered.

2 Mechanical analysis of welded tube in free bending

2.1 Principle of free bending of welded tube

As a new flexible forming technology, three-dimensional free bending technology shows great potential in many industrial fields. The process of free bending of tube was illustrated in Fig. 1. The forming equipment is mainly composed of four parts: bearing, bending die, guider, and feeding device. The outer spherical surface of bending die is matched with the inner spherical surface of the bearing, and the tail of bending die is

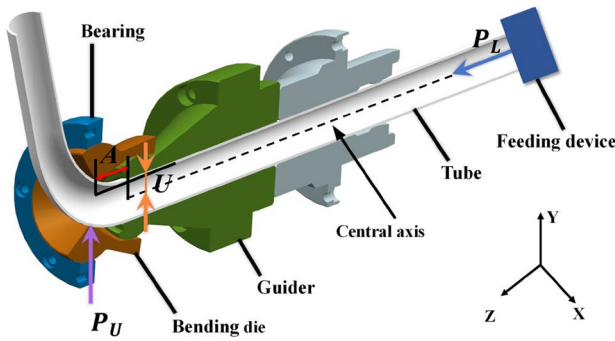


Fig. 1 Schematic diagram of three-dimensional free bending

connected with the head of guider by the special mechanism. Before bending the tube, the centerline of the bending die, bearing, and guider is on the same axis, which coincides with the feed axis of the equipment. During the free bending process, the bending die is in a follow-up state and the tube is always in dynamic contact with the bending die. On the one hand, the center of bending die will move synchronously with the movement of bearing in the X–Y plane. On the other hand, the bending die will rotate around the center of guider when the bending die deviates from the centerline. Therefore, the spatial pose of bending die is determined by the combined motion of the translation in the X–Y plane and the rotation around the guider. In addition, the position of weld can be arbitrarily arranged along the circumferential direction of cross-section of bending die in the free bending process of welded tube.

In the free bending process, the projection distance between the center of bending die and the centerline of guider in the X–Y plane is called as the deflection U . Likewise, the distance between the center of bending die and the exit of guider along the central axis is called as the offset A . The values of A and U together determine the bending moment exerted by the bending die on the bent tube. Specifically, the tube is subjected to the axial force P_L along the Z-axis exerted by the feed device and the radial force P_U perpendicular to the tube axis from the bending die during the free bending process. The combined action of P_L and P_U forms the bending moment M , as shown in Eq. (1), which causes the corresponding bending deformation of the welded tube.

$$M = P_L \times U + P_U \times A \tag{1}$$

2.2 Mechanical analysis of stress–strain

2.2.1 Fundamental assumption

Due to the uneven distribution of the material properties of the welded tube along the circumferential direction, its deformation behavior is very complex during the free bending process. To analyze the influence of welding line on the

plastic deformation behavior of welded tube, some assumptions have been made to simplify the derivation process of the stress–strain equations.

1. The materials in the weld zone and the parent metal zone satisfy the stress–strain relationship, as shown in Eq. (2):

$$\sigma = \begin{cases} E\varepsilon & \text{where } \varepsilon \leq \varepsilon_s \\ \sigma_s + k \times (1 - e^{-m\varepsilon}) & \text{where } \varepsilon \geq \varepsilon_s \end{cases} \tag{2}$$

where E is Young’s modulus, m is hardening exponent, k is a constant, σ is the flow stress, ε is the strain, σ_s is the yield stress, ε_s is the initial plastic strain.

2. The flow of material along the circumferential direction is ignored during the free bending process of welded tube, which can be expressed as:

$$\varepsilon_\varphi = 0 \tag{3}$$

3. The shear stress, shear strain, and thickness stress are ignored and written as:

$$\begin{cases} \sigma_{ij} = 0 (i \neq j) \\ \varepsilon_{ij} = 0 (i \neq j) \end{cases} \tag{4}$$

4. The tube is incompressible during the free bending process. Thus, the following relationship can be satisfied.

$$\varepsilon_\rho + \varepsilon_\theta + \varepsilon_\varphi = 0 \tag{5}$$

5. The friction between the bending die and welded tube is neglected.

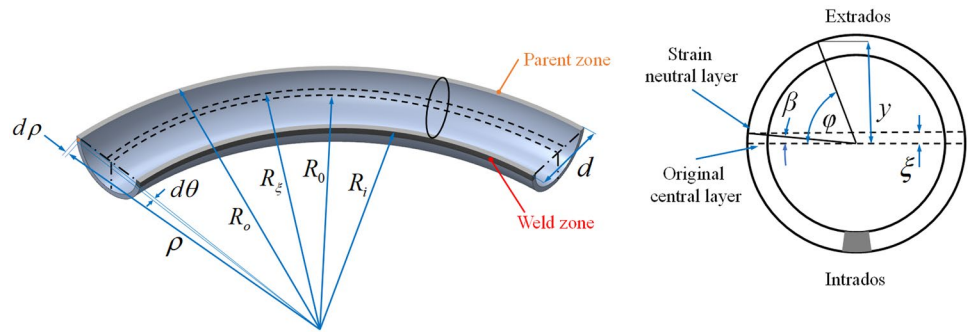
2.2.2 Analysis of stress–strain

During the free bending process of welded tube, the geometric parameters of bent tube between the bending die and guider were described in Fig. 2. The meaning of every symbol was listed in Table 1. The tangential stress–strain (σ_θ - ε_θ), radial stress–strain (σ_ρ - ε_ρ), and circumferential stress–strain (σ_φ - ε_φ) are the principal stress–strain of bent tube. In addition, it is assumed that the welded tube is in the plane strain state, and the relationship between principal stresses can be deduced as Eq. (6) according to the theory of plastic flow.

$$\sigma_\varphi = \frac{\sigma_\theta + \sigma_\rho}{2} \tag{6}$$

According to Hency stress–strain relationship and Eq. (6), the stress equilibrium equation can be expressed as Eq. (7) in the radial direction.

Fig. 2 Geometric parameters of bent tube during the free bending process



$$\frac{d\sigma_\rho}{d\rho} + \frac{\sigma_\rho - \sigma_\theta}{\rho} = 0 \tag{7}$$

Based on the von Mises yield criterion, the equivalent stress and strain of the welded tube during the free bending process can be deduced as Eqs. (8) and (9).

$$\bar{\sigma} = \frac{\sqrt{3}}{2} |\sigma_\theta - \sigma_\rho| \tag{8}$$

$$\bar{\varepsilon} = \sqrt{\frac{2}{3} (\varepsilon_\rho^2 + \varepsilon_\theta^2 + \varepsilon_\varphi^2)} = \frac{2}{\sqrt{3}} |\varepsilon_\theta| \tag{9}$$

Due to the additional axial force P_L exerted on the tube, the strain-neutral layer is shifted from the inside to the outside of the tube. Thus, the tangential strain of the welded tube can be expressed as:

$$\varepsilon_\theta = \frac{(R_\xi + y)d\theta - R_\xi d\theta}{R_\xi d\theta} = \frac{r \sin \varphi - r \sin \beta}{R_0 + r \sin \beta} \tag{10}$$

By substituting Eqs. (8), (9) and (10) into Eq. (2), the following equation was obtained:

$$|\sigma_\theta - \sigma_\rho| = \frac{2}{\sqrt{3}} \left\{ \sigma_s + k \left(1 - e^{-\frac{2}{\sqrt{3}} m \left| \frac{r \sin \varphi - r \sin \beta}{R_0 + r \sin \beta} \right|} \right) \right\} \tag{11}$$

when $\varphi \in [\beta, \pi - \beta]$, $r \sin \varphi - r \sin \beta > 0$; $\varphi \in [\pi - \beta, \beta]$, $r \sin \varphi - r \sin \beta < 0$.

According to Eqs. (7) and (11), the radial stress $\sigma_{\rho i}$ and $\sigma_{\rho o}$ on the inside and outside of bent tube were constructed as:

$$\sigma_{\rho i} = \left\{ -\frac{2}{\sqrt{3}} \left[\sigma_s + k \left(1 - e^{-\frac{2}{\sqrt{3}} m \frac{r \sin \varphi - r \sin \beta}{R_0 + r \sin \beta}} \right) \right] \right\} \ln \rho + C_i \tag{12}$$

$$\sigma_{\rho o} = \left\{ \frac{2}{\sqrt{3}} \left[\sigma_s + k \left(1 - e^{-\frac{2}{\sqrt{3}} m \frac{r \sin \varphi - r \sin \beta}{R_0 + r \sin \beta}} \right) \right] \right\} \ln \rho + C_o \tag{13}$$

where C_i, C_o are the integration constant. Since the radial stress σ_ρ is equal to zero in the extrados surface or intrados surface of bent tube, the radial stress inside and outside of bent tube can be deduced as Eqs. (14) and (15) respectively:

$$\sigma_{\rho i} = \frac{2}{\sqrt{3}} \left[(\sigma_s + k) \ln \frac{R_i}{\rho} + k e^{-\frac{2}{\sqrt{3}} m \left(\frac{r \sin \varphi - r \sin \beta}{R_0 + r \sin \beta} \right)} \ln \rho - k e^{-\frac{2}{\sqrt{3}} m \left(\frac{r - r \sin \beta}{R_0 + r \sin \beta} \right)} \ln R_i \right] \tag{14}$$

$$\sigma_{\rho o} = \frac{2}{\sqrt{3}} \left[(\sigma_s + k) \ln \frac{\rho}{R_o} + k e^{-\frac{2}{\sqrt{3}} m \left(\frac{r + r \sin \beta}{R_0 + r \sin \beta} \right)} \ln R_o - k e^{-\frac{2}{\sqrt{3}} m \left(\frac{r \sin \varphi - r \sin \beta}{R_0 + r \sin \beta} \right)} \ln \rho \right] \tag{15}$$

According to Eqs. (11), (14), and (15), the tangential stress inside and outside of the bent tube can be written as Eqs. (16) and (17) respectively:

Table 1 Definition of every symbol

Symbols	Definitions
R_ξ	The curvature radius of the strain neutral layer of the bent tube
R_0	The curvature radius of the original center layer of the bent tube
R_i, R_o	The curvature radius of the intrados and extrados of the bent tube
ξ	The transverse displacement distance of strain neutral layer in bent tube
β	The displacement angle of strain neutral layer in bent tube
ρ	The curvature radius at any point of the bent tube
y	The distance between any position and the strain neutral layer
$d\theta$	The incremental angle along the tangential direction of bent tube
d, r	The diameter and radius of cross-section of the bent tube
φ	The angle between radius line of cross-section and original central layer

$$\sigma_{\theta_i} = \frac{2}{\sqrt{3}} \left[(\sigma_s + k) \left(\ln \frac{R_i}{\rho} - 1 \right) + ke^{\frac{2}{\sqrt{3}}m \left(\frac{r \sin \varphi - r \sin \beta}{R_0 + r \sin \beta} \right)} (1 + \ln \rho) - ke^{\frac{2}{\sqrt{3}}m \left(\frac{r - r \sin \beta}{R_0 + r \sin \beta} \right)} \ln R_i \right] \tag{16}$$

P_L is large enough, the strain neutral layer will start to

$$\sigma_{\theta_o} = \frac{2}{\sqrt{3}} \left[(\sigma_s + k) \left(\ln \frac{\rho}{R_o} + 1 \right) - ke^{-\frac{2}{\sqrt{3}}m \left(\frac{r \sin \varphi - r \sin \beta}{R_0 + r \sin \beta} \right)} (1 + \ln \rho) + ke^{-\frac{2}{\sqrt{3}}m \left(\frac{r + r \sin \beta}{R_0 + r \sin \beta} \right)} \ln R_o \right] \tag{17}$$

Combining Eqs. (6), (16) and (17), the circumferential stress inside and outside of the bent tube can be derived as (18) and (19) respectively:

move outward along the radial direction, which may be explained by Eq. (20).

$$\sigma_{\varphi_i} = \frac{2}{\sqrt{3}} \left[(\sigma_s + k) \left(\ln \frac{R_i}{\rho} - \frac{1}{2} \right) + ke^{\frac{2}{\sqrt{3}}m \left(\frac{r \sin \varphi - r \sin \beta}{R_0 + r \sin \beta} \right)} \left(\frac{1}{2} + \ln \rho \right) - ke^{\frac{2}{\sqrt{3}}m \left(\frac{r - r \sin \beta}{R_0 + r \sin \beta} \right)} \ln R_i \right] \tag{18}$$

$$\sigma_{\varphi_o} = \frac{2}{\sqrt{3}} \left[(\sigma_s + k) \left(\ln \frac{\rho}{R_o} + \frac{1}{2} \right) - ke^{-\frac{2}{\sqrt{3}}m \left(\frac{r \sin \varphi - r \sin \beta}{R_0 + r \sin \beta} \right)} \left(\frac{1}{2} + \ln \rho \right) + ke^{-\frac{2}{\sqrt{3}}m \left(\frac{r + r \sin \beta}{R_0 + r \sin \beta} \right)} \ln R_o \right] \tag{19}$$

The abovementioned derivation process of the tangential stress, radial stress, and circumferential stress is applicable to the weld zone and parent zone of welded tube. The difference in stress distribution between the weld zone and parent zone can be reflected by changing the coefficients k and m in Eq. (2).

2.3 Analysis on the shift of strain neutral layer

In the free bending process, the additional axial force P_L is uniformly and independently applied to the bent tube along the tangential direction. To maintain the shape of the bent tube, the tangential stress generated by the axial force P_L and bending moment M must satisfy the condition of stress equilibrium. Hence, the following equation can be expressed as:

$$\int_{\pi+\beta}^{2\pi-\beta} \left[\sigma_s + k \left(1 - e^{-m \frac{r \sin \varphi - r \sin \beta}{R_o - r \sin \beta}} \right) \right] r_m t_o d\varphi + \int_{-\beta}^{\pi+\beta} \left[-\sigma_s + k \left(1 - e^{-m \frac{r \sin \varphi - r \sin \beta}{R_o - r \sin \beta}} \right) \right] r_m t_i d\varphi = 0 \tag{20}$$

During traditional bending process of tube (pure bending), to ensure the balance of stress–strain of deformation area, the strain neutral layer keeps moving toward the center of curved arc under the action of bending moment. However, in the process of free bending, the tangential tensile stress on the outside of the bent tube decreases due to the action of additional axial force P_L . In that way, the tendency of the strain neutral layer to shift to the center of curved arc is weakened. When the additional axial force

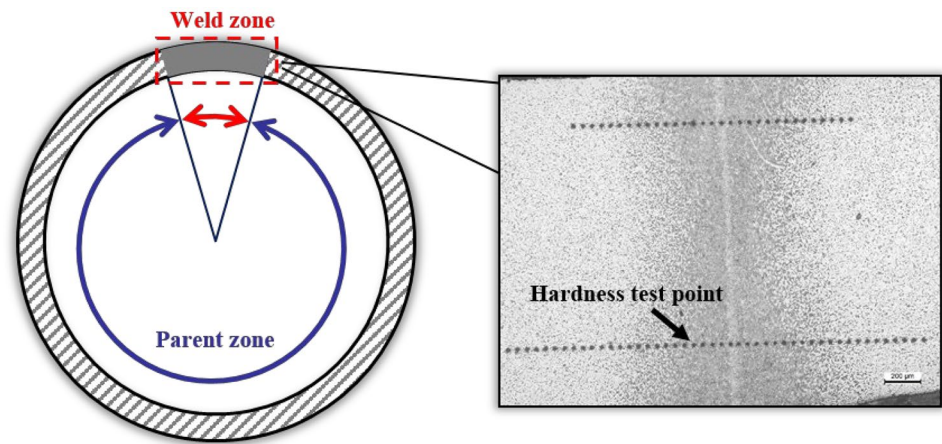
3 Free bending experiment and simulation of welded tube

3.1 Hardness experiment

In this paper, the Q345 welded tube with the diameter of 31.6 mm and the wall thickness of 2 mm was used to study the influence of weld on free bending deformation behavior. Since the mechanical properties of tube in the weld zone are different from those in the parent zone of tube, it is necessary to first determine the distribution area of weld along the circumferential direction in the welded tube. For simplification, the heat-affected zone (HAZ) and welded joint are considered the weld zone in the welded tube. Here the hardness experiment was employed to distinguish the weld zone from the parent zone. The cross-

sectional specimen of welded tube was prepared for the hardness experiment. As shown in Fig. 3, the test points for hardness experiment were evenly distributed along the circumferential direction of tube with the intervals of 0.5 mm, which cover the weld zone and parent zone. To avoid the accidental deviation in the measurement process, the hardness experiments were conducted three times. The microhardness distribution across the weld zone and parent zone of Q345 welded tube was shown in Fig. 4. It

Fig. 3 Hardness experiment of the welded tube



could be found that the microhardness value of weld zone is significantly higher than that of parent zone, and the microhardness value at the centerline of the welded zone is the largest. According to the evolution trend of the microhardness distribution in the weld zone and parent zone of welded tube, the width of weld zone can be determined to be 4 mm, as shown by the fitting curve in Fig. 4.

3.2 Uniaxial tensile test

To accurately determine the mechanical property parameters of weld zone and parent zone in the welded tube, the uniaxial tensile tests for the materials in different zones of welded tube were carried out. The uniaxial tensile specimens in the parent zone were prepared along the axial direction, as shown in Fig. 5a. Due to the narrow weld zone, the uniaxial tensile specimens in the mixed zone containing the weld zone and parent zone were prepared to avoid the impact of cutting on the mechanical properties of the weld, as shown

in Fig. 5a. The geometrical dimension of uniaxial tensile specimen was also illustrated in Fig. 5b.

The flow stress–strain curves of parent zone and mixed zone (parent zone + weld zone) were displayed in Fig. 6. As we can find, the yield stress of the mixed zone is significantly higher than that in the parent zone, which is consistent with the evolution of hardness distribution in Fig. 4. Equation (2) was employed to fit the stress–strain curve of parent zone, and the fitting results were shown in Fig. 6 and Table 2.

To obtain the constitutive model of weld zone, it is necessary to separate the parent zone from the mixed zone, whose principle is shown in Fig. 7. The mixed uniaxial tensile specimen is composed of two parts: parent zone and weld zone. It is assumed that the strain along the tensile direction of parent zone and weld zone is the same during the uniaxial tensile test, which can be expressed as Eq. (21).

$$\varepsilon_m = \varepsilon_p = \varepsilon_w \quad (21)$$

where ε_m is the total strain of the mixed uniaxial tensile specimen, ε_p is the strain of parent zone, and ε_w is the strain of weld zone.

According to the condition of stress equilibrium, the stress relationship between the weld zone and parent zone can be derived as Eq. (22).

$$\sigma_w = \frac{\sigma_m \cdot L_m - \sigma_p \cdot L_p}{L_w} \quad (22)$$

where σ_m and L_m are the stress and width of the mixed zone, σ_p and L_p are the stress and width of the parent zone, σ_w and L_w are the stress and width of the weld zone. Therefore, the flow stress–strain curve of the weld zone can be derived from Eq. (22) and Fig. 6, which was also shown in Fig. 6. In addition, Eq. (2) was used to fit the stress–strain curve of weld zone, and the fitting results were shown in Fig. 6 and Table 2. It was found that the material strength in the weld

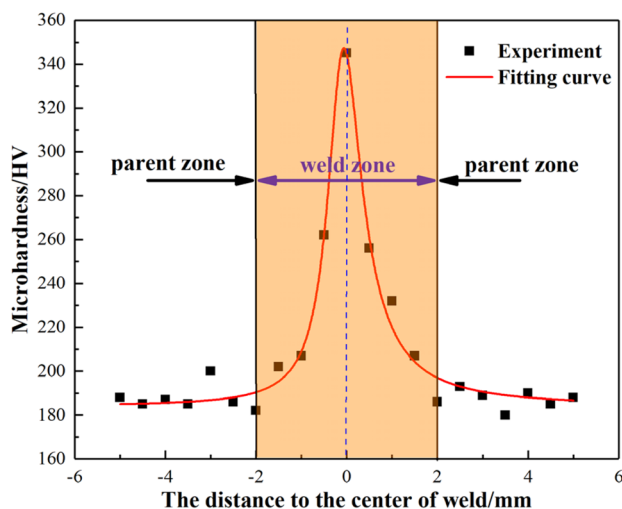
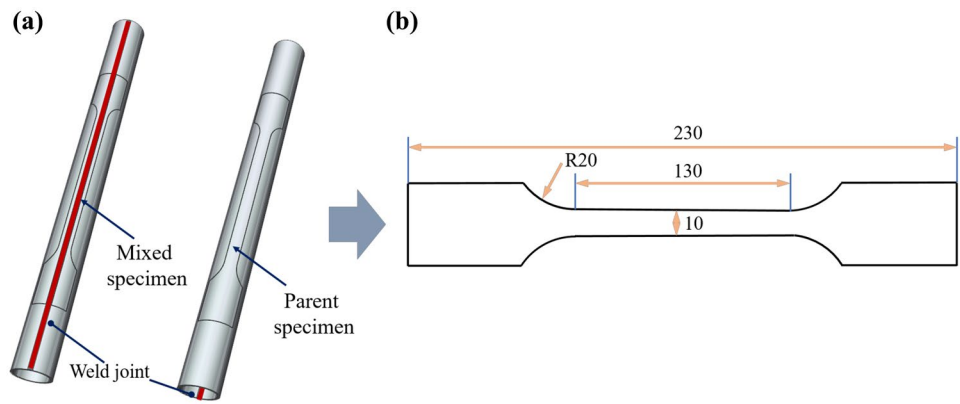


Fig. 4 Microhardness distribution in the weld zone and parent zone

Fig. 5 Uniaxial tensile specimens: **a** specimen taken along the axial direction; **b** geometrical dimension



zone is significantly higher than that in the parent zone and Eq. (2) could accurately describe the flow behavior of parent zone and weld zone of the Q345 welded tube.

3.3 Free bending experiment

The free bending experiment of Q345 welded tube was conducted on the three-axial free bending forming equipment developed by NUAA, as shown in Fig. 8. The inner diameter of bending die is 32 mm in the free bending system. During the free bending process, the welded tube passes through the guider and bending die in turn under the action of feeding device. Since the spatial position and posture of the bending die can be adjusted continuously, the bending radius and angle of bent tube also change

accordingly. Finally, the welded tube is bent into the pre-designed shape under the combined action of the bending die, guider, and feeding device.

Considering that the material mechanical properties of welded tube are unevenly distributed along the circumferential direction of the cross-section and the materials in different zones are in different stress states, it is necessary to study the influence of weld position on the free bending deformation behavior of welded tube. In this paper, the free bending experiments of welded tubes with different weld positions were carried out, and the welds were arranged on the outside, inside and right-side of bent tube, as shown in Fig. 9. The evolution of the bending radius, wall thickness, and cross-sectional distortion with the position of weld was explored by free bending experiments

Fig. 6 The flow stress–strain curves of welded tube

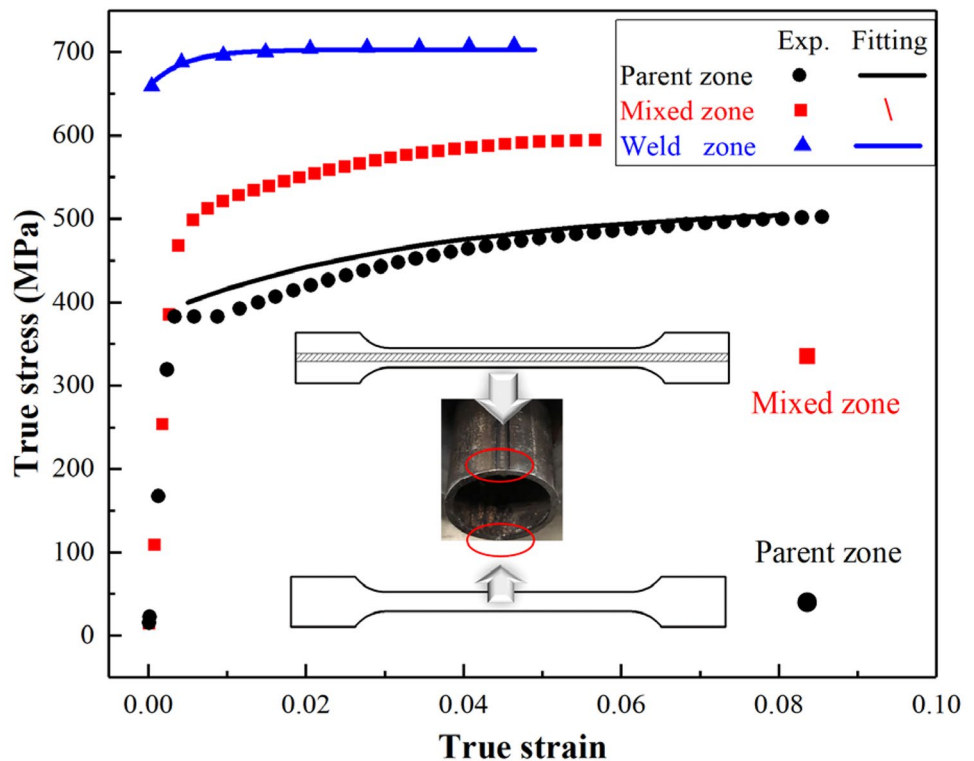


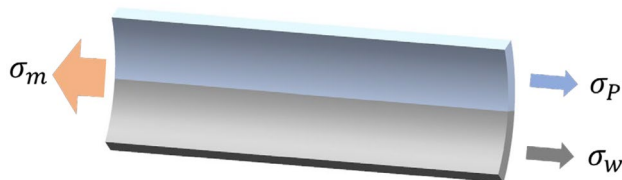
Table 2 Mechanical property parameters in different zones

Zone	σ_s (MPa)	k	m	$COD(R^2)$
Parent zone	381.41	135.16	29.56	0.99985
Mixed zone	501.42	103.87	46.39	0.99874
Weld zone	657.88	44.86	229.30	0.98525

and simulations. The feeding speed of tube and movement speed of bending die were set to be 10 mm/s and 2 mm/s, respectively. To analyze the evolution of bending radius with the deflection U of bending die, the free bending experiments with the deflection U of 4 mm, 6 mm, 8 mm, 10 mm, 12 mm, and 14 mm were implemented. In addition, the lubricating oil was also used between the welded tube and bending die.

3.4 Finite element simulation

To investigate the influence of weld on the free bending deformation behavior of welded tube more deeply and conveniently, the finite element (FE) method was employed to simulate the forming process. As shown in Fig. 10, the 3D FE model was established in the ABAQUS/Explicit platform, which includes the bending die, bearing, guider, and welded tube. Simultaneously, the springback behavior of bent tube was also considered based on the ABAQUS/Standard platform. Due to the uneven distribution of material properties along the circumferential direction of cross-section of welded tube, the weld zone and parent zone should be given different material properties, as listed in Table 2. To balance the simulation accuracy and calculation efficiency, the mesh size of weld zone and parent zone of the welded tube was set to be 1.2 mm and 2.0 mm, respectively. The tube was meshed by 4-node shell elements (S4R). Considering that the bending die, bearing, and guider hardly undergo plastic deformation during the free bending process, they were dispersed by C3D10M solid elements and defined as rigid bodies. The interaction between different modules was set to be the general contact. Since the lubrication oil was used between the bending die and tube, the friction coefficient was set to be 0.02. Other simulation process parameter settings can be determined according to the free bending forming experiment. In addition, the free bending

**Fig. 7** Stress distribution of the mixed uniaxial tensile specimen

deformation behavior of Q345 tube without welding line was also simulated numerically, and the mechanical properties of parent zone were assigned to the whole tube.

4 Results and discussion

According to the previous analysis, the mechanical properties of weld zone are significantly different from those in the parent zone. The different areas of tube along the circumferential direction are in different stress states during free bending process. The coupling effect between the non-uniform distribution of the material and the stress state of tensile-compression makes the free bending deformation behavior of welded tube more complicated. In this paper, the influence of weld position on the distribution of wall thickness, U - R relationship, and cross-sectional distortion was explored by free bending experiments and numerical simulations. In addition, the free bending deformation behavior of seamless tube was also analyzed. Here, four typical weld positions were discussed: the outside of the bending direction (WOD), the right-side of the bending direction (WRD), the inside of the bending direction (WID), and tube without weld (non-weld).

4.1 Comparison of simulation and experimental results

To explore the influence of weld on the free bending deformation behavior of welded tube, the results of free bending of welded tube and seamless tube need to be compared. Due to the lack of Q235 seamless tube, the free bending forming process of seamless tube may be characterized by the finite element numerical simulation. Therefore, it is necessary to first verify the feasibility of numerical simulation method. The finite element numerical simulation and experiment of free bending of welded tube were conducted and the corresponding bent tubes were shown in Fig. 11a. The deflection U of bending die was set to be 6 mm, and the weld was arranged on the right-side of the bending direction. It was found that the shape of the simulated bent tube is close to that of the experimental bent tube and the bending radius obtained by simulation is slightly larger than the experimental result. This may be due to the fact that the mechanical properties of welded tube are unevenly distributed along the axial and circumferential directions of tube. In addition, the simulation result of free bending of seamless tube was also compared in Fig. 11b. The simulated bending radii of welded and seamless tubes are almost the same. Hence, it could be preliminarily concluded that the free bending forming process of seamless tube can be accurately described by numerical simulation. The positional relationship between the welding line and strain neutral layer was depicted in

Fig. 8 Three-axial free bending forming equipment

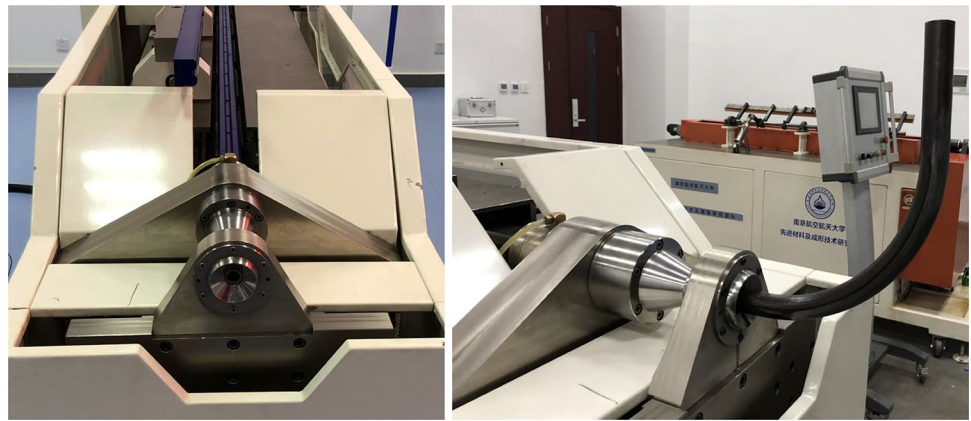


Fig. 12. It was found that the strain neutral layer is very close to the welding line, and the influence of the weld on the plastic deformation behavior of welded tube could be ignored during the free bending process.

In addition, the wall thickness distribution of the simulated and experimental bent tubes was shown in Fig. 13. When the weld is located on the right-side of the bending direction, the numerical simulation results of the welded tube and seamless tube are almost identical, and are relatively close to the experimental results. The increase in the wall thickness of the intrados of bent tube is significantly higher than the reduction in the wall thickness of the extrados of bent tube, which is attributed to the fact that the axial force P_L along the Z-axis suppresses the thinning of the outer wall thickness. The above analysis shows that the free bending forming process of welded tube and seamless tube can be reasonably characterized by the numerical simulation method.

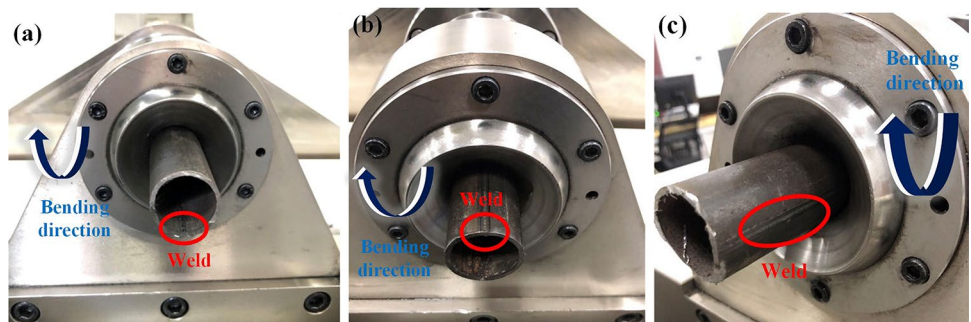
4.2 Influence of weld position on U-R relationship

Due to the inconsistency of mechanical properties between the weld zone and parent zone of welded tube and the different stress states inside and outside of bent tube during the free bending process, the plastic deformation behavior and springback evolution law of welded tube are very complicated, which further affects the axial shape and size of the bent tube. The experimental bent tubes with different

deflection U were shown in Fig. 14, whose welds were arranged on the right-side of the bending direction. The relationships between the bending radius of bent tube R and the deflection U of bending die under different weld positions conditions were also summarized in Fig. 14b. It could be found that the position of weld has a significant influence on the U - R relationship when the deflection U of bending die is relatively small. When the weld of welded tube is located on the inside, outside and right-side of bending direction, respectively, the corresponding bending radius decreases in sequence under the condition of the same deflection U . In addition, the numerical simulation result of free bending of seamless tube was also shown in Fig. 14, which is close to the case where the weld is located on the right-side of bending direction. However, the weld position hardly affects the U - R relationship when the deflection U of bending die is relatively large.

The influence of weld position on the U - R relationship of welded tube could be analyzed and explained from the perspective of the springback of bent tube and the distribution of stress-strain. According to the conclusions of previous research, the mechanical properties of material have an impact on the springback behavior of component, and the degree of springback increases with increasing yield strength and strain hardening index. The simulated bent tubes with different weld positions were shown in Fig. 15 when the deflection U of bending die was set as 6 mm. The stress in the weld zone is significantly higher than that in the

Fig. 9 Free bending experiments of welded tube with different weld positions: **a** outside of bent tube; **b** inside of bent tube; **c** right-side of bent tube



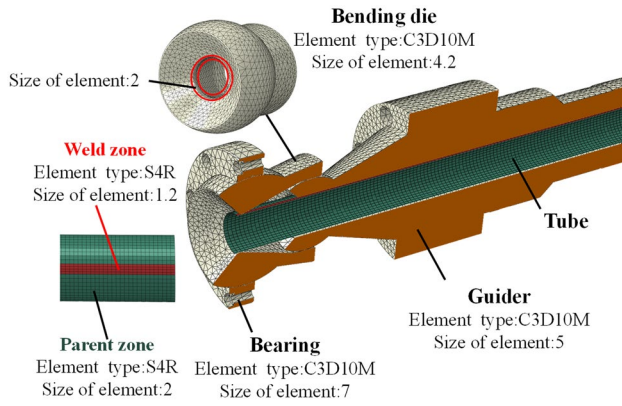


Fig. 10 FE model of free bending of welded tube

parent zone when the weld is located on the inside or outside of bending direction. Thus, the springback of bent tube with the outside or inside weld is significantly larger than that with the right-side weld, resulting in an increase in the bending radius. Considering that the weld on the right-side of bending direction hardly undergoes plastic deformation during the free bending process, the weld has little effect on the springback behavior of the welded tube, and the experimental results are close to the numerical simulation results of the seamless tube.

In addition, the plastic strain inside the bent tube is greater under the action of axial thrust, resulting in more obvious springback behavior when the weld is located on the inside of bending direction. With the increase in the

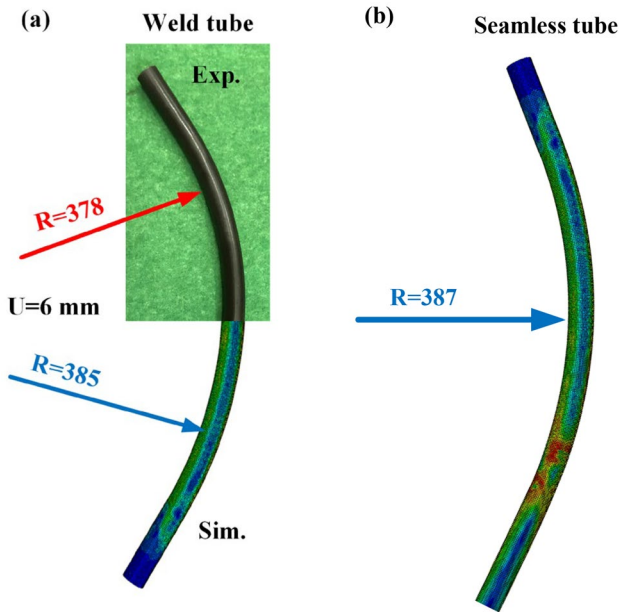


Fig. 11 Comparison of the experimental and simulation bent tubes: **a** experimental and simulation bent tube with weld; **b** simulation bent tube without weld

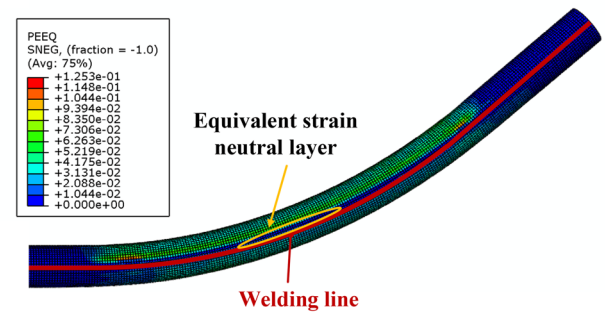


Fig. 12 The positional relationship between the welding line and strain neutral layer

deflection U of bending die, the deformation degree of welded tube increases, and the proportion of elastic strain in the total strain decreases. Thus, the shape and size of the bent tube are less affected by the springback behavior, and the influence of the weld position on the bending radius of welded tube could be ignored. When the weld is located on other position, the U - R relationship curve should lie between the U - R curves of WRD and WOD (or WID).

4.3 Influence of weld position on cross-sectional distortion

To quantitatively describe the influence of the weld position on the cross-sectional distortion, the cross-sectional distortion rate γ was introduced to reflect the flattening degree of tube, as shown in Fig. 16, which was defined as:

$$\gamma = \frac{d_{\max} - d_{\min}}{d_0} \times 100\% \tag{23}$$

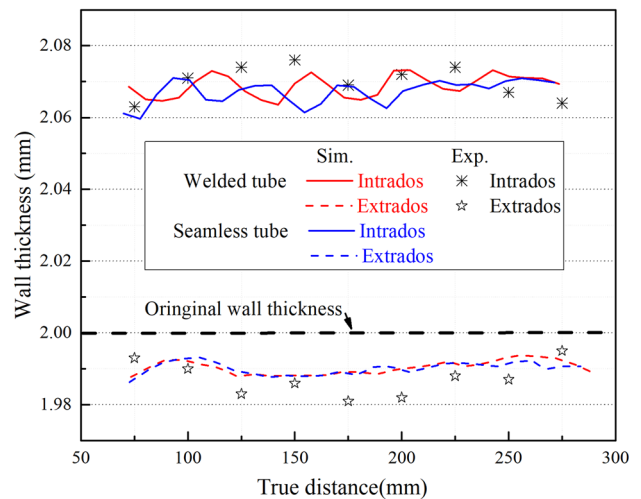
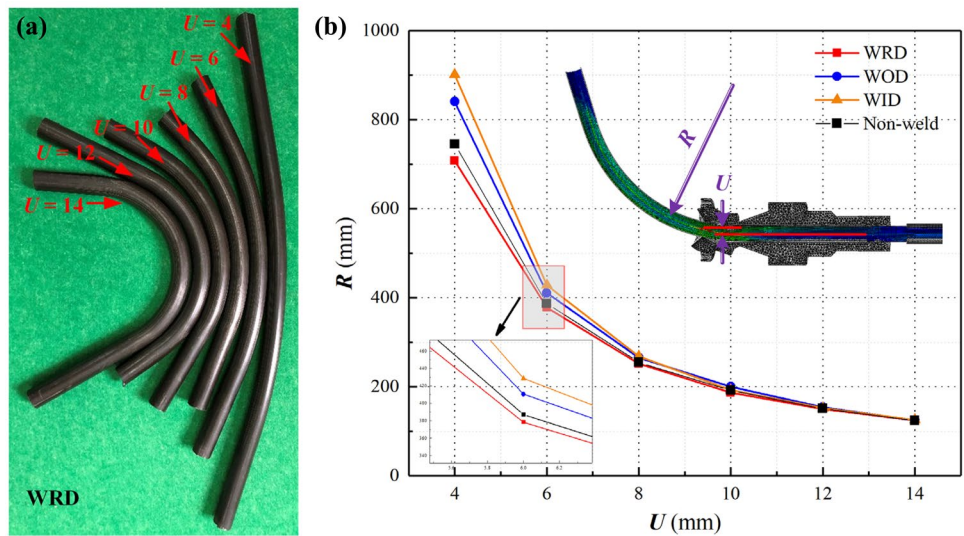


Fig. 13 Wall thickness distribution of welded and seamless tubes

Fig. 14 U - R relationships of welded tube and seamless tube: **a** experimental bent tube; **b** U - R relationship curves



where d_0 is the initial diameter of welded tube, d_{max} and d_{min} are the maximum and minimum diameters of the cross-section of bent tube, respectively.

The evolution law of cross-sectional distortion rate γ with the deflection U of bending die was obtained by free bending experiments under different weld position conditions, which was shown in Fig. 17. The cross-sectional distortion rate γ of the seamless tube obtained by the numerical simulation method was also compared in Fig. 17. It should be clarified that the cross-section of bent tube used to measure the

cross-sectional distortion rate is located in the stable arc part to avoid the influence of the unstable elements on the forming result. The cross-sectional distortion rate of the bent tube increases with increasing the deflection U of bending die, which can be attributed to that the severe plastic deformation of tube under a larger deflection U would further aggravate the flattening degree of bent tube. In addition, when the weld of welded tube is located on the inside, outside and right-side of bending direction respectively, the corresponding cross-sectional distortion rate γ decreases in

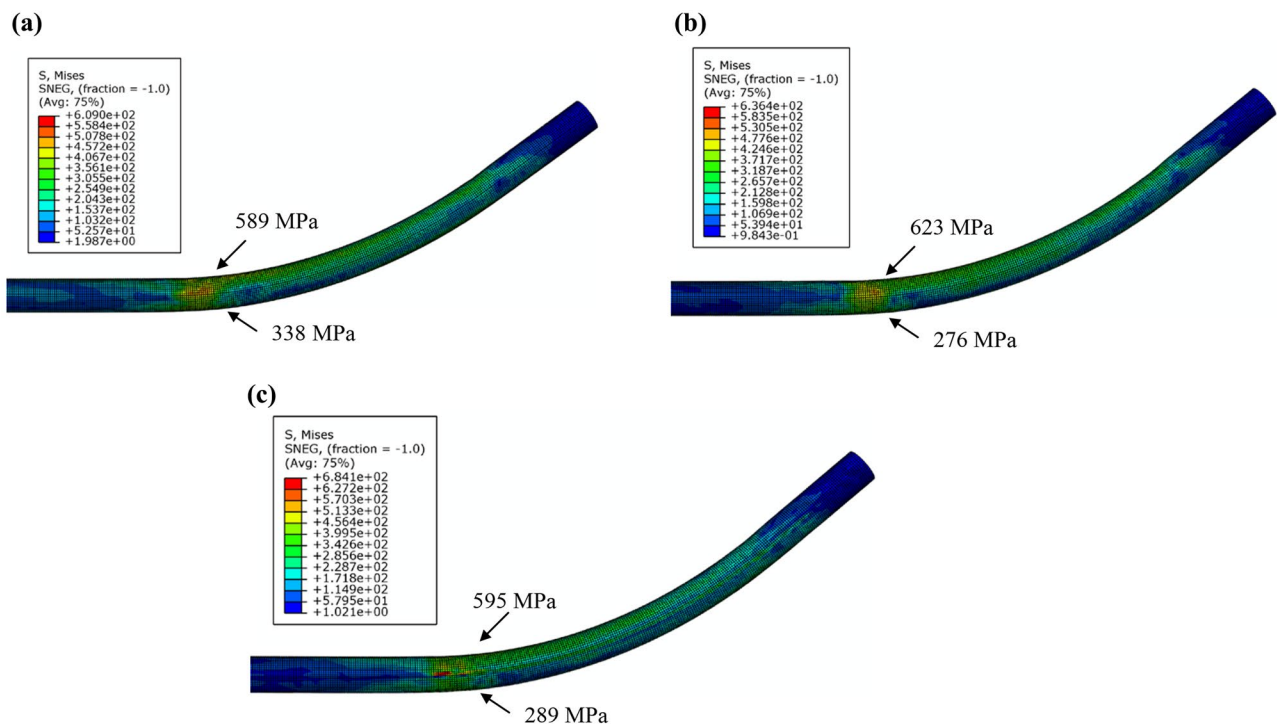


Fig. 15 The simulated bent tubes with different weld positions: **a** outside of bent tube; **b** inside of bent tube; **c** right-side of bent tube

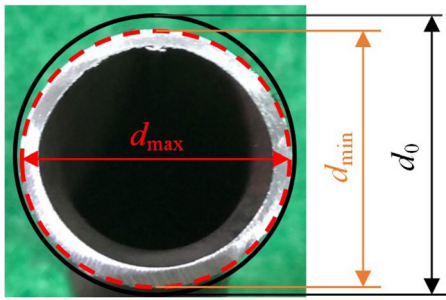


Fig. 16 Schematic diagram of measuring the cross-sectional distortion rate

sequence under the condition of the same deflection U . Furthermore, the effect of weld position on the cross-sectional distortion rate γ might be ignored when the deflection U is small. Compared with the case where the weld is located on the outside or inside of bending direction, the cross-sectional distortion rate γ of welded tube with the right-side weld is almost consistent with the numerical simulation results of the seamless tube.

In the process of free bending, the stress state and cross-sectional deformation of bent tube were schematically depicted in Fig. 18. By analyzing the distribution of tangential stress in the process of bending, the tube is bent under the action of bending moment M . The resultant force (N_1, N_2) of tangential tensile stress $\sigma_{\theta o}$ on the outside of bent tube and tangential compressive stress $\sigma_{\theta i}$ on the inside of bent tube points to the center of cross-section of bent tube, causing the flattening deformation of tube along the directions of N_1 and N_2 . Since the yield stress of material in the weld zone is larger than that in the parent zone, it can be deduced from Eqs. (16) and (17) that the tangential compressive stress or tangential

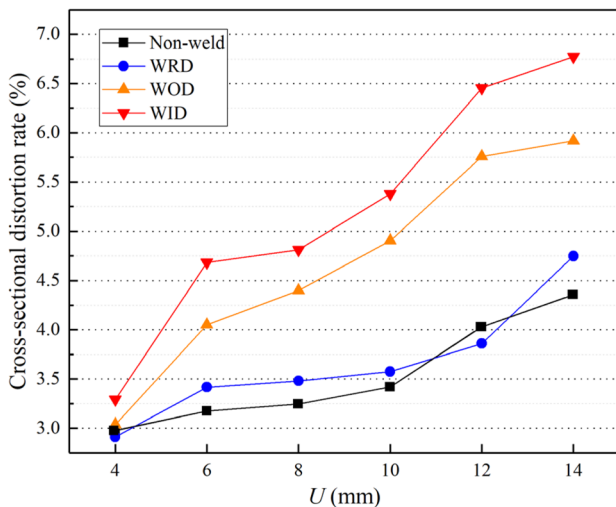


Fig. 17 Cross-sectional distortion rate of the bent tube under different deflection U

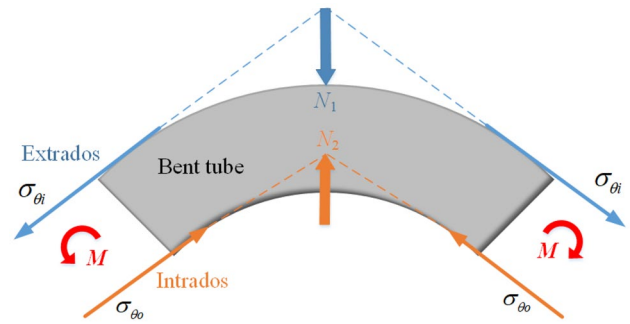


Fig. 18 Schematic diagram of cross-sectional deformation of bent tube

tensile stress in the weld zone is greater than that in the parent zone under the same deformation condition. When the weld is located on the outside or inside of bending direction, the deformation resistance of tube is greater and the larger resultant N_1 or N_2 would cause more severe cross-sectional distortion. In addition, the cross-sectional distortion rate γ of welded tube with the inside weld is greater than that with the outside weld, which can be attributed to the fact that the tangential compressive stress on the inside of bending direction is larger than the tangential tensile stress on the outside of bending direction under the action of axial force P_L . When the weld is located on the right-side of bending direction, the weld zone is close to the position of the strain-neutral layer, and the plastic deformation of weld zone could be ignored. Thus, the cross-sectional distortion rate γ of welded tube with the right-side weld is almost consistent with the numerical simulation results of the seamless tube.

4.4 Influence of weld position on the wall thickness distribution

The evolution of the wall thickness distribution of welded tube with the weld position under different deflection U conditions was obtained by the finite element simulation, which was depicted in Fig. 19. The wall thickness was measured from the stable arc segment of bent tube, and the true distance refers to the length from the starting position of the curved arc segment. Moreover, the experimental results of the wall thickness distribution of welded tube with the right-side weld were also supplemented in Fig. 19 to demonstrate the reliability of the numerical simulation results. It was found that the increase in the wall thickness of the intrados of bent tube is significantly higher than the reduction in the wall thickness of the extrados of bent tube. With the increase in the deflection U , the thinning of the wall thickness of the extrados and the thickening of the wall thickness of the intrados become more obvious. In addition, when the weld is located on the outside of the bending direction, the thickening of intrados of welded tube and the thinning of extrados

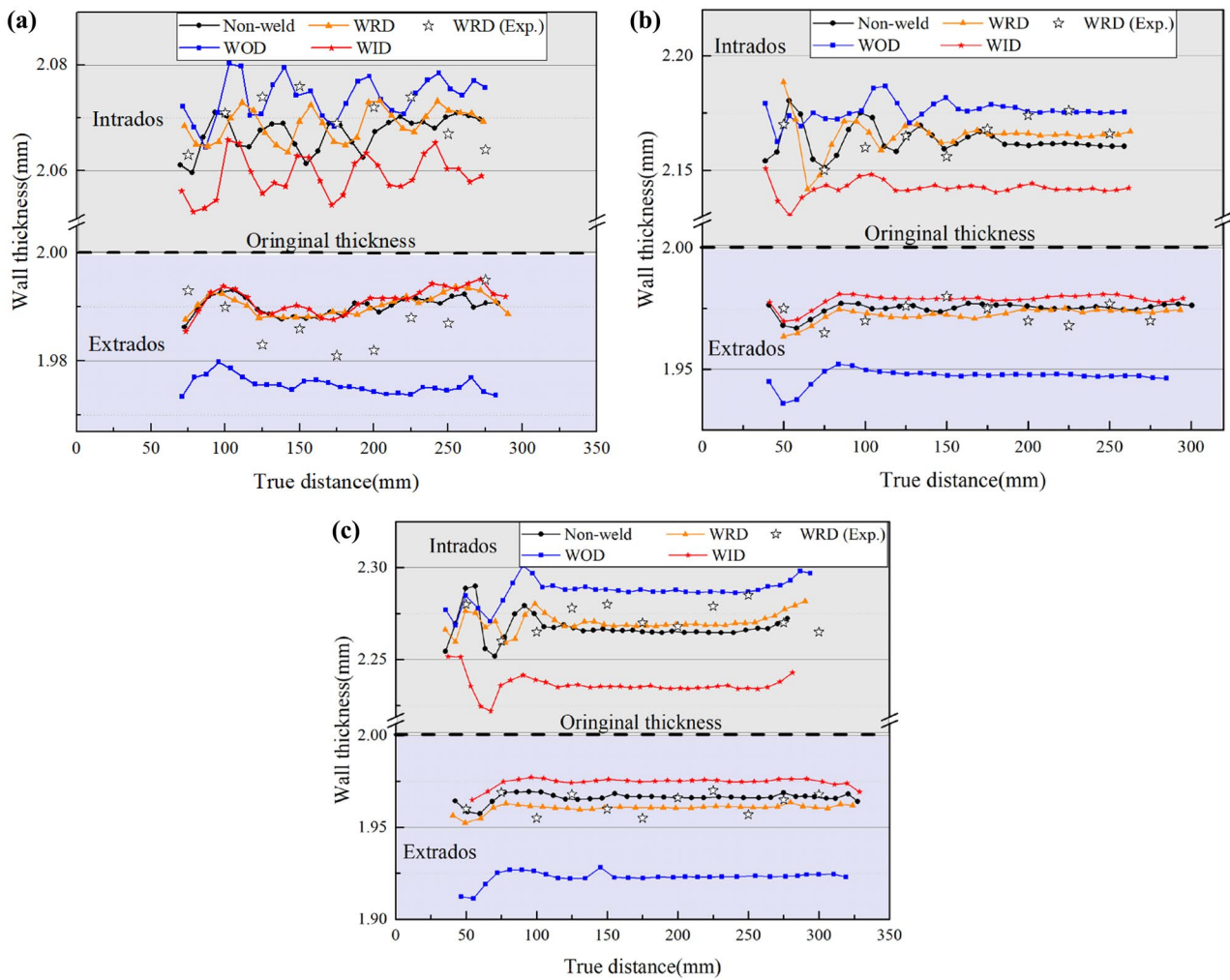


Fig. 19 Comparison of the wall thickness distribution with different weld positions: **a** $U=6$ mm; **b** $U=10$ mm; **c** $U=14$ mm

of welded tube become more severe. Compared with the results of free bending of welded tube with the right-side weld, the thickening of the wall thickness of the intrados and the thinning of the wall thickness of the extrados would be weakened when the weld is located on the inside of bending direction. Moreover, the wall thickness distribution of the seamless tube is basically consistent with the results of free bending of welded tube with the right-side weld. Hence, it could be concluded that the influence of weld on the change in wall thickness is very significant when the weld is located on the outside of bending direction, resulting in a more uneven wall thickness distribution of the welded tube. When the weld is located on the inside of bending direction, the thickening of intrados and the thinning of extrados of bent tube would be suppressed, and the uniformity of thickness distribution of welded tube could be improved.

To explain the evolution law of the wall thickness distribution of welded tube with the weld position, the theory of strain neutral layer shift and the phenomenon of

cross-sectional distortion would be introduced. When the weld is located at the outside of bending direction, it can be deduced that the strain neutral layer would tend to shift from the intrados to extrados according to Eq. (20). Thus, the wall thickness thickening in the intrados of bent tube would be promoted. Regardless of the circumferential strain, the tangential tensile strain of extrados of bent tube is approximately equal to the strain along the thickness direction of bent tube. Considering that the cross-sectional distortion rate γ of welded tube with the outside weld is less than that with the inside weld during the free bending process, the excessive thinning of the extrados of welded tube with the outside weld could be determined. Similarly, the strain neutral layer would tend to shift from the extrados to intrados according to Eq. (20) when the weld is located at the inside of bending direction. The wall thickness thickening in the intrados of bent tube would be suppressed. Furthermore, the wall thickness thinning of the extrados of bent tube would also be suppressed due to the larger cross-sectional distortion

rate γ . When the weld is located at the right-side of bending direction, there is almost no plastic deformation in the weld zone and the bending deformation behavior of welded tube is similar to that of the seamless tube. Therefore, the wall thickness distribution of intrados and extrados of welded tube is consistent with that of the seamless tube.

5 Conclusion

In this paper, the influence of weld on the deformation behavior of welded tube during the free bending process was sufficiently explored. The constitutive model of welded tube was established by hardness tests and uniaxial tensile tests. The influence of weld position on the U - R relationship, cross-sectional distortion, and wall thickness distribution was analyzed. The main findings were summarized in the following:

1. The material strength in the weld zone of welded tube is significantly higher than that in the parent zone. The mechanical properties and constitutive models of the weld zone and parent zone are considered and modeled separately.
2. The weld position has a significant influence on the U - R relationship. When the weld of welded tube is located at the inside, outside and right-side of bending direction respectively, the corresponding bending radius decreases in sequence. In the free bending process of welded tube, the influence of weld position on the shape of bent tube needs to be considered.
3. When the weld is located at different positions, the evolution law of the cross-sectional distortion rate γ of welded tube with the deflection U of bending die is different. The cross-sectional distortion rate γ of welded tube is the smallest when the weld is arranged on the right-side of bent tube.
4. The thickening of wall thickness of intrados and the thinning of wall thickness of extrados of bent tube would be suppressed when the weld is located at the inside of bending direction and the uniformity of thickness distribution of welded tube could be improved. Therefore, to improve the forming quality and axis dimensional accuracy of welded tube in the free bending process, the weld position needs to be carefully considered.

Author contribution All authors contributed to the study conception and design. Material preparation, data collection, and analysis were performed by Cheng Cheng, Chao Pan, Xueshan Bai. The first draft of the manuscript was written by Chunmei Liu and Xunzhong Guo. The revised manuscript was finished by Cheng Cheng and Xunzhong Guo. All authors commented on previous versions of the manuscript. All authors read and approved the final manuscript.

Funding This work was supported by the Opening Project of State Key Lab of Digital Manufacturing Equipment & Technology (No. DMETKF2021004), the National Natural Science Foundation of China (Nos: 52105360, U1937206), Ningbo “science and technology innovation 2025” major special project (No.2020Z078), and Youth Fund of Jiangsu Province Natural Science Foundation (No.BK20210310).

Declarations

Competing interests The authors declare no competing interests.

References

1. Song H, Xie W, Zhang S, Jiang W, Lăzărescu L, Banabic D (2021) Granular media filler assisted push bending method of thin-walled tubes with small bending radius. *Int J Mech Sci* 198:106365. <https://doi.org/10.1016/j.ijmecsci.2021.106365>
2. Zhan M, Guo K, Yang H (2016) Advances and trends in plastic forming technologies for welded tubes. *Chinese J Aeronaut* 29(2):305–315. <https://doi.org/10.1016/j.cja.2015.10.011>
3. Borchmann L, Frohn-Sörensen P, Engel B (2020) In situ detection and control of wrinkle formation during rotary draw bending. *Procedia Manuf* 50:589–596. <https://doi.org/10.1016/j.promfg.2020.08.106>
4. Lukassen TV, Gunnarsson E, Krenk S, Glejbøl K, Lyckegaard A, Berggreen C (2019) Tension-bending analysis of flexible pipe by a repeated unit cell finite element model. *Mar Struct* 64:401–420. <https://doi.org/10.1016/j.marstruc.2018.09.010>
5. Wang A, Xue H, Saud S, Yang Y, Wei Y (2019) Improvement of springback prediction accuracy for Z-section profiles in four-roll bending process considering neutral layer shift. *J Manuf Process* 48:218–227. <https://doi.org/10.1016/j.jmapro.2019.11.008>
6. Yang H, Li H, Zhang Z, Zhan M, Liu J, Li G (2012) Advances and trends on tube bending forming technologies. *Chinese J Aeronaut* 25(1):1–12
7. Gantner P, Harrison DK, De Silva AK, Bauer H (2007) The development of a simulation model and the determination of the die control data for the free-bending technique. *Proc Inst Mech Eng Part B J Eng Manuf* 221(2):163–171. <https://doi.org/10.1243/09544054JEM642>
8. Wu J, Zhang Z, Shang Q, Li F, Wang Y, Hui Y, Fan H (2017) A method for investigating the springback behavior of 3D tubes. *Int J Mech Sci* 131–132:191–204. <https://doi.org/10.1016/j.ijmecsci.2017.06.047>
9. Beulich N, Craighero P, Volk W (2017) FEA simulation of free-bending – a preforming step in the hydroforming process chain. *J Phys Conf Ser* 896(1). <https://doi.org/10.1088/1742-6596/896/1/012063>
10. He Y, Jing Y, Mei Z, Heng L, Yongle K (2009) 3D numerical study on wrinkling characteristics in NC bending of aluminum alloy thin-walled tubes with large diameters under multi-die constraints. *Comp Mater Sci* 45(4):1052–1067. <https://doi.org/10.1016/j.commatsci.2009.01.010>
11. Guo X, Xiong H, Xu Y, El-Aty AA, Ma Y, Zhao Y, Zhang S (2018) U-R relationship prediction method for aluminum alloy circular tube free-bending process based on sensitivity analysis of material parameters. *Int J Adv Manuf Technol* 99(5):1967–1977. <https://doi.org/10.1007/s00170-018-2614-5>
12. Ren N, Zhan M, Yang H, Zhang ZY, Qin YT, Jiang HM, Diao KS, Chen XP (2012) Constraining effects of weld and heat-affected zone on deformation behaviors of welded tubes in numerical control bending process. *J Mater Process Tech* 212(5):1106–1115. <https://doi.org/10.1016/j.jmatprotec.2011.12.023>

13. Ren N, Yang H, Zhan M, Zhang ZY (2013) Strain distribution characteristics of welded tube in NC bending process using experimental grid method. *Int J Adv Manuf Technol* 66(5–8):635–644
14. Liu H, Liu Y, Zhang P, Du X (2020) Effect of weld zone and corner with cold bending effect on wrinkling of rectangular welded tube in rotary draw bending. *Thin Wall Struct* 157:107115. <https://doi.org/10.1016/j.tws.2020.107115>
15. Zhan M, Xing L, Gao PF, Ma F (2019) An analytical springback model for bending of welded tube considering the weld characteristics. *Int J Mech Sci* 150:594–609. <https://doi.org/10.1016/j.ijmecsci.2018.10.060>
16. Khalfallah A (2014) Experimental and numerical assessment of mechanical properties of welded tubes for hydroforming. *Mater Des* 1980–2015(56):782–790
17. Xing L, Zhan M, Gao PF, Ma F (2018) A method for establishing a continuous constitutive model of welded metals. *Mater Sci Eng A* 718:228–240. <https://doi.org/10.1016/j.msea.2018.01.062>
18. Omar A, Tewari A, Narasimhan K (2020) Effect of bulge ratio on the deformation behaviour and fracture location during welded steel tube hydroforming process. *Results Mater* 6:100096. <https://doi.org/10.1016/j.rinma.2020.100096>
19. Jang Y, Lee Y, Song M, Han D, Kim N, Lee H (2021) Evaluation of ductile fracture in welded tubes with tensile, hardness, flaring tests. *Int J Mech Sci* 210:106745. <https://doi.org/10.1016/j.ijmecsci.2021.106745>
20. Liu H, Liu Y (2021) Cross section deformation of heterogeneous rectangular welded tube in rotary draw bending considering different yield criteria. *J Manuf Process* 61:303–310

Publisher's note Springer Nature remains neutral with regard to jurisdictional claims in published maps and institutional affiliations.